NEOPLASIA
www.neoplasia.com

Volume 15 Number 9 September 2013 pp. 1100–1109 1100

# Tumor Microenvironmental Signaling Elicits Epithelial-Mesenchymal Plasticity through Cooperation with Transforming Genetic Events[1]

**Damian J. Junk*, Rocky Cipriano*, Benjamin L. Bryson*, Hannah L. Gilmore*,† and Mark W. Jackson*,‡**

*Department of Pathology, Case Western Reserve University, Cleveland, OH; †University Hospitals Case Medical Center, Case Western Reserve University, Cleveland, OH; ‡Case Comprehensive Cancer Center, Case Western Reserve University, Cleveland, OH

## Abstract

Epithelial-to-mesenchymal transition (EMT) facilitates the escape of epithelial cancer cells from the primary tumor site, which is a key event early in metastasis. Here, we explore how extrinsic, tumor microenvironmental cytokines cooperate with intrinsic, genetic changes to promote EMT in human mammary epithelial cells (HMECs). Viral transduction of transforming genetic events into HMECs routinely generated two distinct cell populations. One population retained epithelial characteristics, while an emergent population spontaneously acquired a mesenchymal morphology and properties associated with cancer stem cells (CSCs). Interestingly, the spontaneous mesenchymal/CSCs were unable to differentiate and lacked epithelial-mesenchymal plasticity. In contrast, exposure of the transformed HMECs retaining epithelial characteristics to exogenous transforming growth factor–β (TGF-β) generated a mesenchymal/CSC population with remarkable plasticity. The TGF-β–induced mesenchymal/CSC population was dependent on the continued presence of TGF-β. Removal of TGF-β or pharmacologic or genetic inhibition of TGF-β/SMAD signaling led to the reversion of mesenchymal/CSC to epithelial/non-CSC. Our results demonstrate that targeting exogenous cytokine signaling disrupts epithelial-mesenchymal plasticity and may be an effective strategy to inhibit the emergence of circulating tumor cells. The model of epithelial-mesenchymal plasticity we describe here can be used to identify novel tumor microenvironmental factors and downstream signaling that cooperate with intrinsic genetic changes to drive metastasis. Understanding the interaction between extrinsic and intrinsic factors that regulate epithelial-mesenchymal plasticity will allow the development of new therapies that target tumor microenvironmental signals to reduce metastasis.

*Neoplasia (2013) 15, 1100–1109*

## Introduction

Metastasis is the cause of breast cancer fatality [1]. Metastasis consists of four steps, namely, invasion and entry of primary tumor cells into the circulatory system, survival of circulating tumor cells (CTCs), movement from the circulation into a secondary tissue, and tumor growth at a secondary site [2]. The changes that occur in cancer cells that allow them to accomplish these steps and metastasize remain poorly understood.

Epithelial-to-mesenchymal transition (EMT) occurs during normal organism development, wound healing, and formation of branched tissue, such as lung or breast [3–6]. In normal breast tissue, tight cell-cell interactions anchor epithelial cells to each other creating a physical hindrance to cell dispersal and a natural barrier to metastasis [7,8]. It has been proposed that epithelial tumor cells undergo EMT,

Abbreviations: AIG, anchorage-independent growth; CSC, cancer stem cell; CTC, circulating tumor cell; DN–TAK-1, dominant negative TGF-β–activated kinase 1; DN-TGFβRII, dominant negative TGF-β receptor type II; EMT, epithelial-to-mesenchymal transition; HMECs, human mammary epithelial cells; LY, PI3K inhibitor LY294002; qRT-PCR, quantitative real-time reverse transcription–polymerase chain reaction; RAP, rapamycin; SB, TGF-β receptor type I inhibitor SB431542

Address all correspondence to: Mark W. Jackson, PhD, Case Western Reserve University, 2103 Cornell Road, WRB 3134, Cleveland, OH 44106. E-mail: mark.w.jackson@case.edu

[1]This research was supported by the Athymic Animal and Xenograft, Tissue Procurement and Histology, Cytometry and Imaging Microscopy, and Radiation Resources Core Facilities of the Case Comprehensive Cancer Center (P30 CA43703). This work was supported by the US National Institutes of Health (R01CA138421 to M.W.J.; T32CA059366 to R.C. and D.J.J.) and the American Cancer Society (Research Scholar Award No. RSG CCG-122517). The authors declare no conflicts of interest.
Received 30 May 2013; Revised 25 July 2013; Accepted 30 July 2013


DOI 10.1593/neo.131114

releasing mesenchymal-like cells that are motile and invasive and can initiate metastasis [9,10]. While EMT allows release of tumor cells from primary cancer sites, evidence supports that a reciprocal mesnchymal-to-epithelial transition occurs at distant sites [11]. Thus, metastasis requires that a tumor cell gain the capacity to transition between epithelial and mesenchymal states. Epithelial-mesenchymal plasticity would allow epithelial tumor cells in the primary tumor to acquire invasive and survival programs associated with a mesenchymal state, escape from the primary tumor, survive as a CTC, and then revert to an epithelial state at secondary sites.

The regulation of epithelial-mesenchymal plasticity is likely to be dependent on non-tumor cells in the tumor microenvironment, which include a variety of tumor-associated stromal cells, such as fibroblasts, infiltrating immune cells, and endothelial cells [12]. As a tumor develops, changes occur not only in the epithelial tumor cells but also in nearby tumor-associated stromal cells. Indeed, analysis of breast tumor stroma identified elevated levels of a variety of growth factors, cytokines, and chemokines compared to normal breast stroma [13]. However, it remains unclear how each of these tumor-associated factors influences tumor cell growth and epithelial-mesenchymal plasticity.

Seminal work demonstrated that EMT of transformed human mammary epithelial cells (HMECs) generates mesenchymal-like cells with properties associated with breast cancer stem cells (CSCs) [14]. Breast CSCs are identified by a $CD24^-/CD44^+$ cell surface marker profile [15]. When sorted from breast cancer tumors, $CD24^-/CD44^+$ cells generate a variety of differentiated progeny and form tumors that recapitulate the histology of the patients' primary tumors [15]. In contrast, $CD24^+/CD44^-$ cells are unable to efficiently form tumors and are referred to as non-CSCs. The ability of epithelial/non-CSC to undergo EMT and acquire CSC properties is now believed to play a role in therapeutic resistance and metastasis.

The current study demonstrates that exogenous cytokine signaling from the tumor microenvironment can cooperate with defined, intrinsic genetic changes to generate tumor cell plasticity. Exogenous cytokine exposure converted epithelial/non-CSC to mesenchymal/CSC through activation of EMT. Interestingly, maintenance of mesenchymal/CSC required continuous exposure to cytokine, as removal caused reversion to an epithelial/non-CSC population. Generation and maintenance of mesenchymal/CSC could be blocked by disrupting components of endogenous cytokine signaling. The results presented here suggest that targeting epithelial-mesenchymal plasticity may be an effective strategy to reduce tumor formation, progression, and metastasis leading to improved patient outcomes. As such, epithelial-mesenchymal plasticity can be disrupted by targeting the epithelial tumor cells as described here or inhibiting the generation of soluble factors by the tumor-associated stromal cells.

## Materials and Methods

### *Cell Growth*

HMECs were obtained from discarded surgical material under Institutional Review Board (IRB) approval. Specimen 48R, specimen J (SJ), and derivatives were grown as described previously [16,17]. Treatments were 10 ng/ml human recombinant transforming growth factor–β1 (TGF-β1, 100-21; PeproTech Inc, Rocky Hill, NJ), 5 μM phosphoinositide 3-kinase (PI3K) inhibitor LY294002 (LY, 70920; Cayman Chemical, Ann Arbor, MI), 100 mM mammalian target of rapamycin (mTOR) inhibitor rapamycin (RAP, 553210; EMD Millipore, Billerica, MA), and 20 μM TGF-β receptor type I (TGFβRI) inhibitor SB431542 (SB; S4317; Sigma-Aldrich, St Louis, MO). Soft agar assays were described previously [16,18].

### *Viral Infections*

48R HMECs were transduced as previously described [16]. SJ HMECs were transduced similarly, except pRetroSUPER-shp53-puro was used [19]. Kinase dead dominant negative TGF-β–activated kinase 1 (DN–TAK-1) cDNA, dominant negative TGF-β receptor type II (DN-TGFβRII), and SMAD7 were cloned into pLPCX (631511; Clontech, Mountain View, CA) [20–22].

### *Microscopy*

Bright-field images were captured at ×4 on a Nikon Eclipse TE2000-S using MetaMorph (Molecular Devices, Sunnyvale, CA). For confocal analyses, $1.5 \times 10^5$ cells were plated onto 35-mm glass bottom microwell dishes (P35G-1.5-20-C; MatTek Corp, Ashland, MA) for growth overnight. Cells were fixed and permeabilized in 100% methanol and stained overnight with 1:50 dilutions of E-cadherin (clone 67A4, SC-21791-AF647) and vimentin (clone V9, SC-6260-AF488; Santa Cruz Biotechnology, Santa Cruz, CA). Nuclei were counterstained with 50 μg/ml Hoechst dye. Images were captured by oil immersion at ×100 on a Zeiss LSM 510 using AIM software.

### *Flow Cytometry*

Cells ($2 \times 10^6$) were stained with 20 μl of epithelial cell adhesion molecule (EpCAM)–fluorescein isothiocyanate (clone VU-1D9; STEMCELL Technologies, Vancouver, BC) or 20 μl each of CD24-phycoerythrin (PE) (clone ALB9, IM1428U; Beckman Coulter, Brea, CA) and CD44-allophycocyanin (APC) (clone C26, 559942; BD Biosciences, San Jose, CA) for analysis on LSRII using FACSDiva version 6.2 software (Becton Dickinson, San Jose, CA).

### *Western Blot Analysis*

Western blots were conducted as described previously [16]. Antibodies used were E-cadherin (clone 67A4, SC-21791), vimentin (clone V9, SC-6260; Santa Cruz Biotechnology), and actin (ACTN05, MS-1295; Thermo Scientific, Waltham, MA).

### *Quantitative Real-Time Reverse Transcription–Polymerase Chain Reaction*

Total ribonucleic acid (RNA) was isolated using an RNeasy Mini Kit (Qiagen, Valencia, CA) with on-column DNase I digest. RNA (1 μg) was reverse transcribed by $RT^2$ First Strand Kit (C-03/330401). The $RT^2$ Profiler PCR Array System (SABiosciences, Frederick, MD) for EMT (PAHS-090D) and TGF-β/bone morphogenetic protein (BMP) signaling pathway (PAHS-035D) was analyzed on a CFX96 thermocycler (Bio-Rad, Hercules, CA).

### *Phospho-Kinase Arrays*

A Proteome Profiler Human Phospho-Kinase Array Kit (ARY003; R&D Systems, Minneapolis, MN) was used according to the manufacturer's instructions.

### *Mouse Xenografts*

Animal studies were approved by the Case Western Institutional Animal Care and Use Committee. Cells ($1 \times 10^6$) were flank injected with 50% growth factor–reduced Matrigel (353261; BD Biosciences) in NCR nu/nu mice irradiated 4 hours previously with 400 rad. Tumors were resected at 12 weeks, fixed with formalin, paraffin

embedded, sliced, mounted to slides, and stained with hematoxylin and eosin. Images were captured at ×400 on an Olympus BX45 with a SPOT Idea camera (software version 5). One tumor was dissociated overnight using collagenase (C0130) and hyaluronidase (H3506; Sigma-Aldrich). Infiltrating mouse cells were eliminated by selection with 200 μg/ml G418.

## Results

### *Transformation of HMECs Generates a Subset of Mesenchymal-Like Cells through EMT*

Starting with normal HMECs from elective breast reduction mammoplasty, we have developed a genetically defined, stepwise protocol to achieve consistent transformation. Specimen 48R HMECs were infected with viruses encoding short hairpin RNA (shRNA) targeting p16 then p53 (48R-shp16-shp53). 48R-shp16-shp53 populations were subsequently infected with retroviruses encoding RAS alone, MYC alone, MYC and RAS together (M/R), or a vector control retrovirus. Each of the derivatives was plated in soft agar (200,000 cells/plate) to assess anchorage-independent growth (AIG). Robust AIG of 48R HMECs was only observed when all four genetic events were combined together (Figure 1*A*). Interestingly, a population of cells with a spindle-shaped morphology, indicative of mesenchymal-like cells, emerged within the 48R-shp16-shp53–M/R cells (48-Mixed; Figure 1*B*, *top panel*). The cells with mesenchymal-like morphology (48-Mesenchymal) were weakly attached to the substratum and could be separated from the epithelial cells (48-Epithelial) by differential trypsinization (Figure 1*B*, *bottom panels*).

Flow cytometry was used to determine the expression of the epithelial cell surface marker EpCAM in each of the isolated populations.

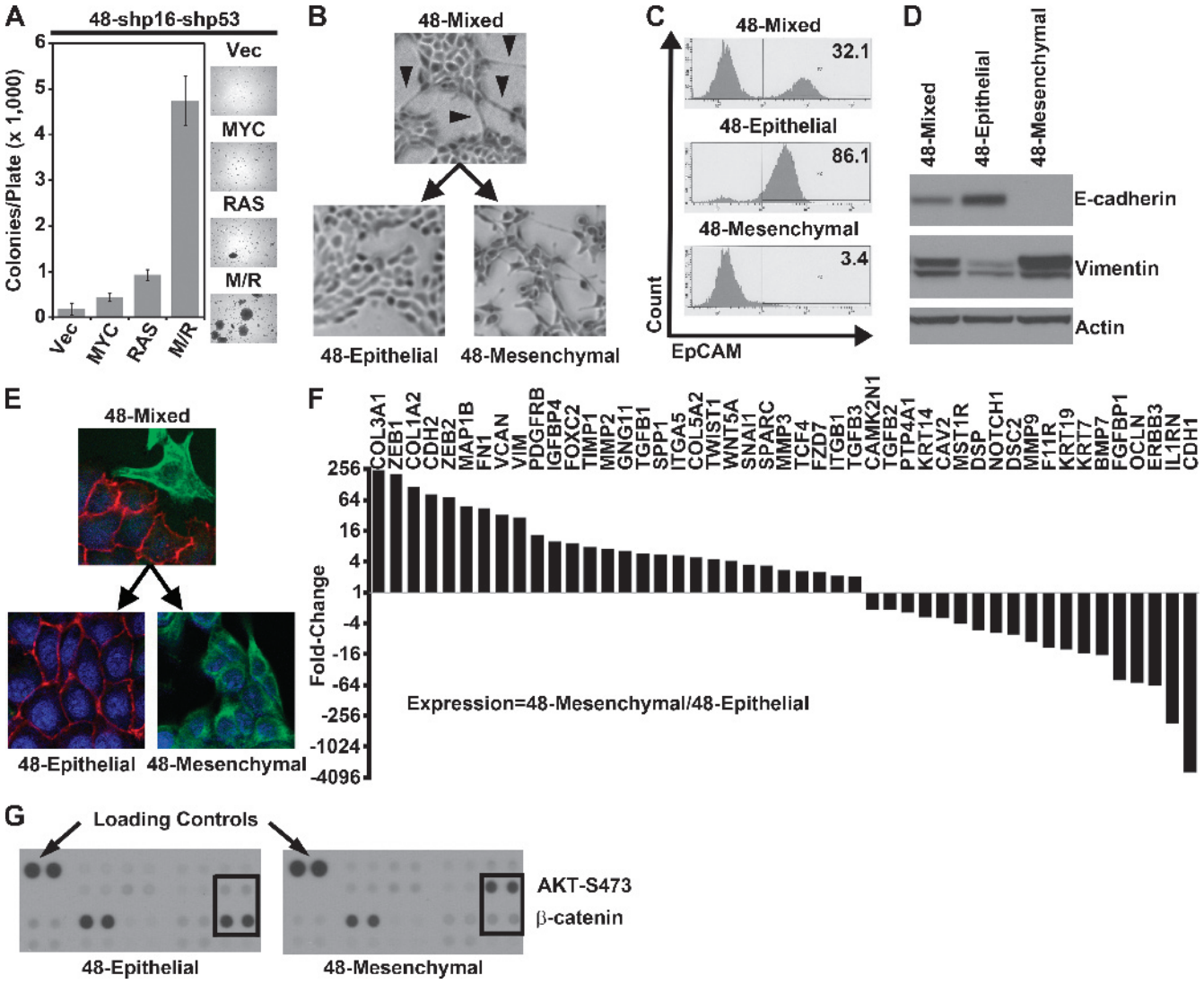


**Figure 1.** HMEC transformation generates a subset of mesenchymal-like cells through EMT. 48-shp16-shp53 HMECs were further infected with control retrovirus (Vec) or retroviruses encoding MYC alone (MYC), RAS alone (RAS), or MYC and RAS together (M/R). (A) Quantification of AIG. (B) Bright-field microscopy (×4) of 48R-shp16-shp53–M/R cells (48-Mixed) revealed cells with mesenchymal-like morphology (arrowheads). The mesenchymal-like cells (48-Mesenchymal) could be separated from the epithelial cells (48-Epithelial) by differential trypsinization. Characterization of the 48-Mixed, 48-Epithelial, and 48-Mesenchymal cells by (C) analysis of EpCAM, (D) Western blot, (E) confocal microscopy (×100) for E-cadherin (red), vimentin (green), and nuclei (blue), (F) EMT-related gene expression changes, and (G) phospho-protein differences.

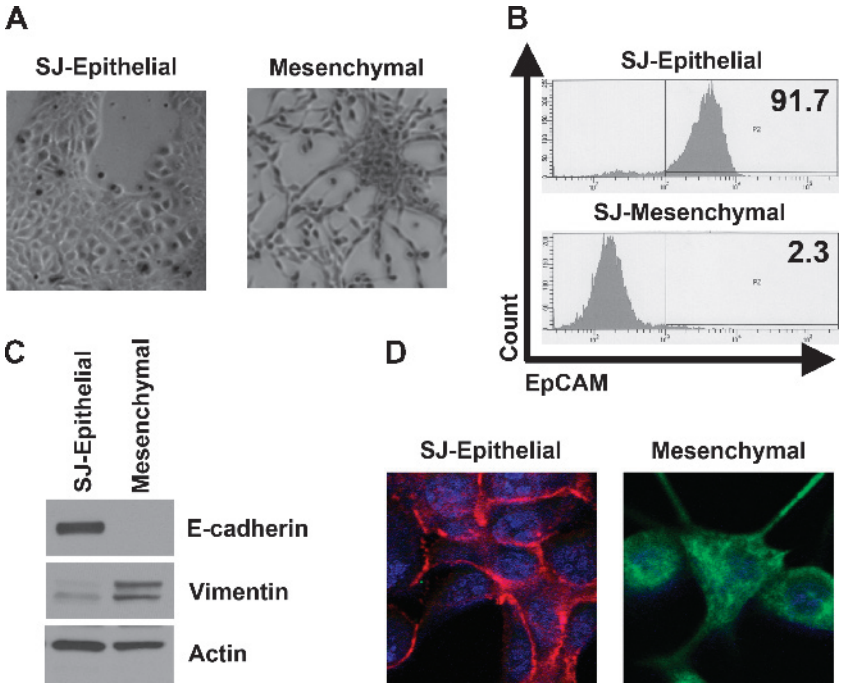


**Figure 2.** Spontaneous EMT is a common consequence of HMEC transformation. SJ HMECs were transformed as in Figure 1. (A) Bright-field microscopy (×4) of epithelial (SJ-Epithelial) and mesenchymal-like (SJ-Mesenchymal) populations separated by differential trypsinization. The SJ-Epithelial and SJ-Mesenchymal cells were analyzed by (B) flow cytometry for EpCAM, (C) Western blot analysis, or (D) confocal microscopy (×100) for E-cadherin (red), vimentin (green), and nuclei (blue).

The 48-Epithelial population was 86.1% positive for EpCAM, while only 3.4% of the 48-Mesenchymal population expressed EpCAM (Figure 1*C*). Thus, the 48-Mixed cells consisted of two isogenic cell populations with epithelial-like and mesenchymal-like morphologies that could be isolated from one another with greater than 85% purity by differential trypsinization.

Because the 48-Mixed cells consisted of both epithelial- and mesenchymal-like cellular morphologies, we hypothesized that a spontaneous EMT had occurred during transformation to generate the 48-Mesenchymal population. To test this hypothesis, the 48-Mixed, 48-Epithelial, and 48-Mesenchymal populations were characterized for known markers of EMT. Western blot and confocal analyses demonstrated that the epithelial marker E-cadherin is expressed in the 48-Epithelial cells, while the mesenchymal marker vimentin is expressed in the 48-Mesenchymal cells with mutual exclusivity (Figure 1, *D* and *E*). The 48-Epithelial and 48-Mesenchymal cells were subjected to a targeted EMT quantitative real-time reverse transcription–polymerase chain reaction (qRT-PCR) array, which confirmed the loss of E-cadherin gene transcription in the 48-Mesenchymal population as well as decreased expression of genes whose loss is associated with EMT, such as caveolin 2, occludin, desmocollin 2, and keratin 19 among others (Figure 1*F*). In addition, qRT-PCR confirmed increased gene transcription of vimentin in the 48-Mesenchymal population as well as increased gene expression of snail, twist, zeb1, and zeb2, among others, all known arbiters of EMT (Figure 1*F*).

Previous studies have demonstrated that EMT of transformed HMECs requires canonical and non-canonical WNT signaling [23]. The EMT expression array confirmed increases in components of WNT signaling (WNT5a, TCF4, and FZD7) in the 48-Mesenchymal population compared to the expression levels in the 48-Epithelial population (Figure 1*F*). In addition to the targeted EMT expression array, the 48-Epithelial and 48-Mesenchymal populations were subjected to analysis of protein phosphorylation using a targeted phospho-kinase antibody array. Increased AKT phosphorylation at serine 473 was evident in the 48-Mesenchymal population, indicating that mTOR signaling is activated (Figure 1*G*). Additionally, β-catenin total phosphorylation was diminished in the 48-Mesenchymal population. Since phosphorylation of β-catenin marks it for degradation, this suggests that the 48-Mesenchymal population harbors increased β-catenin levels and activity.

To verify that the spontaneous EMT identified in 48R HMECs was a general consequence of HMEC transformation and not a patient-specific artifact, HMECs isolated from a second patient that had undergone a reduction mammoplasty were subjected to the genetically defined, stepwise transformation protocol. HMECs from SJ were virally transduced with the same transforming genetic events. Like the transformed 48R HMECs, a population of cells with a spindle-shaped morphology indicative of mesenchymal cells emerged within the transformed SJ-shp16-shp53–M/R epithelial cells. The cells with mesenchymal-like morphology (SJ-Mesenchymal) were separated from the epithelial cells (SJ-Epithelial) by differential trypsinization (Figure 2*A*). Flow cytometry determined that the SJ-Epithelial population was 91.7% positive for the epithelial marker EpCAM, while only 2.3% of the SJ-Mesenchymal population expressed EpCAM (Figure 2*B*). Western blot and confocal analyses again confirmed that the epithelial marker E-cadherin is expressed exclusively in the SJ-Epithelial cells, while the mesenchymal marker vimentin is expressed in the SJ-Mesenchymal cells (Figure 2, *C* and *D*). These data suggest that inhibiting the tumor suppressors p16 and p53 while expressing the oncogenes *MYC* and *RAS* efficiently drives AIG. During this genetically defined, stepwise transformation protocol, a population of cells with mesenchymal-like morphology that can be separated from the epithelial cell population emerges.

### *Mesenchymal-Like Cells Have Properties Associated with Breast CSCs*

Previous reports have demonstrated that EMT generates cells with properties associated with CSC phenotypes including a $CD24^{-}/CD44^{+}$ surface marker profile [14]. Thus, we hypothesized that the spontaneous EMT that occurred during HMEC transformation would generate breast CSCs. To test this hypothesis, 48-Mixed, 48-Epithelial, and 48-Mesenchymal cells were characterized for CD24 and CD44 cell surface marker expression. Flow cytometry revealed that the 48-Epithelial cells consisted primarily of a $CD24^{+}/CD44^{-}$ population indicative of a non-CSC population (epithelial/non-CSC), while the separated 48-Mesenchymal cells consisted primarily of a $CD24^{-}/CD44^{+}$ population indicative of a CSC population (mesenchymal/CSC) (Figure 3*A*). Similar results were obtained using the SJ-Epithelial and SJ-Mesenchymal cells (Figure 3*B*).

A property associated with CSCs is their ability to generate tumors with few cells. To determine if the 48-Mesenchymal and SJ-Mesenchymal cells acquired characteristics of CSCs compared to the 48-Epithelial and SJ-Epithelial cells, each cell type was plated in

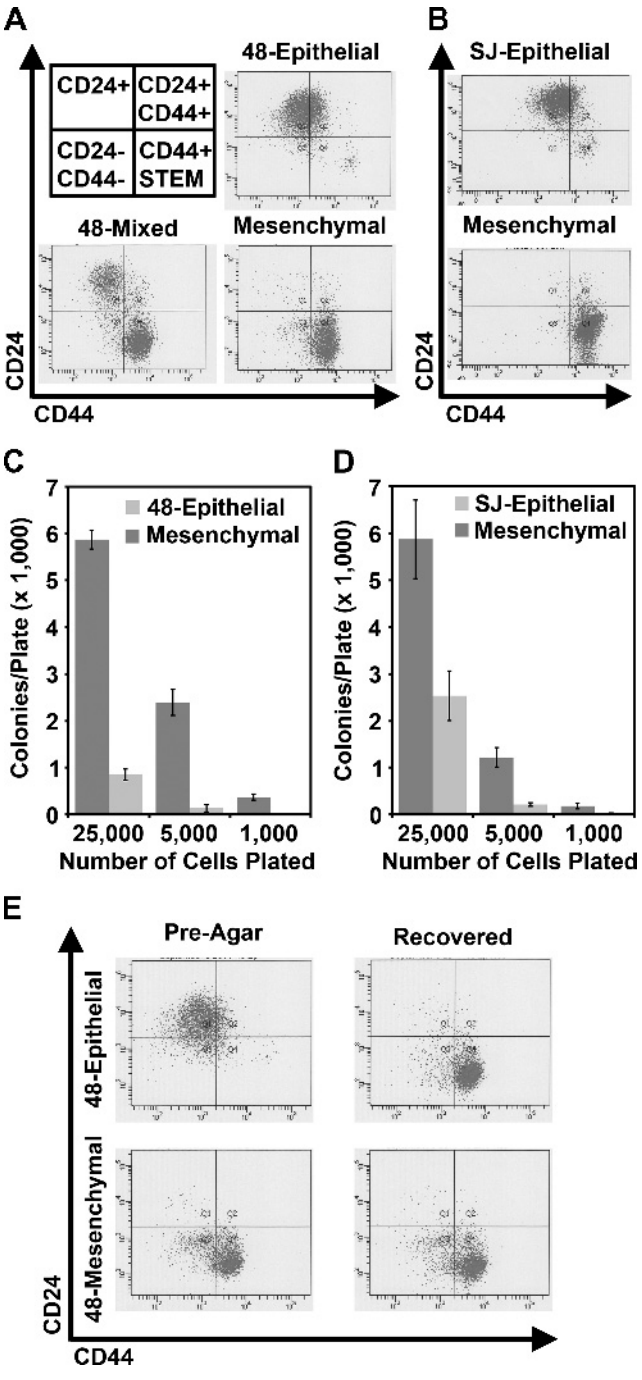


**Figure 3.** Mesenchymal-like cells acquire properties of CSCs. (A) 48-Mixed, 48-Epithelial, and 48-Mesenchymal cells and (B) SJ-Epithelial and SJ-Mesenchymal cells were analyzed by flow cytometry for CD24 and CD44 expression. AIG of (C) 48-Mesenchymal and 48-Epithelial cells and (D) SJ-Mesenchymal and SJ-Epithelial cells was assessed at diminishing cell numbers. (E) Flow cytometry of 48-Epithelial and 48-Mesenchymal cells before (Pre-agar) and after (Recovered) AIG.

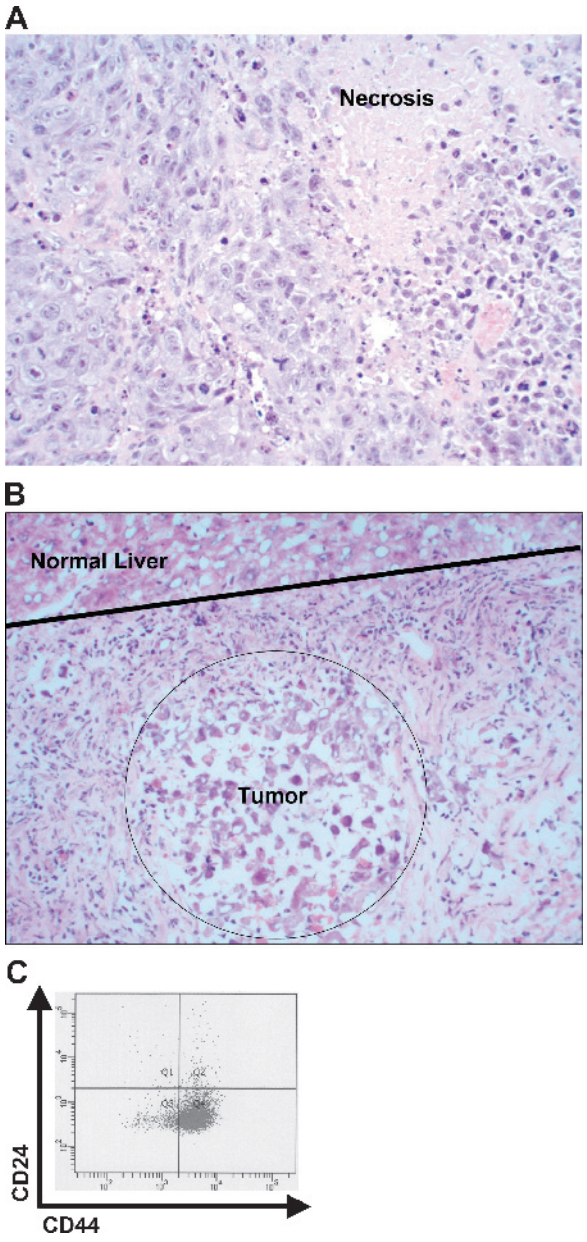


**Figure 4.** Mesenchymal-like cells form tumors *in vivo*. Representative hematoxylin and eosin staining (×400) of (A) a primary tumor and (B) a liver tumor formed by 48-Mesenchymal cells. (C) Flow cytometry of cells cultured from a primary tumor xenograft.

soft agar at diminishing cell number to assess AIG. At low plating densities, the 48-Mesenchymal and SJ-Mesenchymal cells formed nearly 10 times more colonies than their epithelial counterparts (Figure 3, *C* and *D*). To verify that AIG is associated with a CSC profile, we recovered soft agar colonies generated by 48-Mesenchymal and 48-Epithelial populations and demonstrated that recovered cells had a $CD24^-/CD44^+$ CSC surface marker profile, regardless of the starting profile of the cells (Figure 3*E*). These results suggest that AIG is associated with a $CD24^-/CD44^+$ CSC profile.

Since the 48-Mesenchymal cells grew well in agar at limiting dilutions and demonstrated a breast CSC profile, we hypothesized that these cells would generate tumors in immune-compromised mice. 48-Epithelial or 48-Mesenchymal populations were injected into athymic nude mice, and tumors were resected at 12 weeks. The 48-Epithelial cells did not form any tumors *in vivo*, while five tumors were formed from six injections of the 48-Mesenchymal cells, consistent with their ability for AIG and their $CD24^-/CD44^+$ CSC surface marker profile. 48-Mesenchymal xenograft tumors were high-grade carcinoma with extensive necrosis, a large degree of nuclear pleomorphism, and numerous atypical mitotic figures, consistent with poorly differentiated breast cancer (Figure 4*A*). One macroscopic liver tumor was generated by the 48-Mesenchymal cells. The liver tumor was also poorly differentiated similar to the primary flank tumors (Figure 4*B*). One primary tumor was dissociated for tissue culture growth. Analysis of the cultured cells revealed a $CD24^-/CD44^+$ CSC profile (Figure 4*C*). These data demonstrate that only the transformed cells with a $CD24^-/CD44^+$ CSC profile were capable of forming tumors in mice consistent with their ability for AIG in limiting dilutions. Interestingly, the tumors formed were poorly differentiated and maintained a $CD24^-/CD44^+$ CSC profile, suggesting that these cells were incapable of differentiation, inconsistent with a stem cell phenotype.

### *Autocrine and Paracrine Cytokine Signaling Generate Mesenchymal/CSC through EMT*

TGF-β signaling induces EMT in HMEC transformation models [23,24]. Consistent with these observations, the targeted EMT qRT-PCR array analysis demonstrated that TGF-β1 and TGF-β3 were elevated in the 48-Mesenchymal cells (Figure 1*F*). Therefore, we hypothesized that TGF-β signaling played a significant role in the spontaneous EMT observed during HMEC transformation. A targeted TGF-β superfamily signaling pathway qRT-PCR array was used to identify differences in TGF-β superfamily gene expression between 48-Epithelial and 48-Mesenchymal cells. Of 84 TGF-β superfamily target genes on the array, 34 (40%) were differentially expressed more than two-fold between the 48-Epithelial and 48-Mesenchymal cells. This analysis confirmed the induction of TGF-β1 and TGF-β3 gene expression in the 48-Mesenchymal cells, as well as increased gene expression of the type I and type III TGF-β receptors (Figure 5*A*). A number of the related bone morphogenetic protein ligand genes including *BMP2*, *BMP4*, *BMP5*, and *growth differentiation factor 5* (*GDF5*), as well as the bone morphogenetic protein receptor, type IB (BMPR1B) receptor (Figure 5*A*), were also increased in the 48-Mesenchymal cells. The expression of the activin ligand inhibitors INHA and INHBA were decreased in the 48-Mesenchymal cells compared to their 48-Epithelial counterparts (Figure 5*A*). These data suggest that the spontaneously

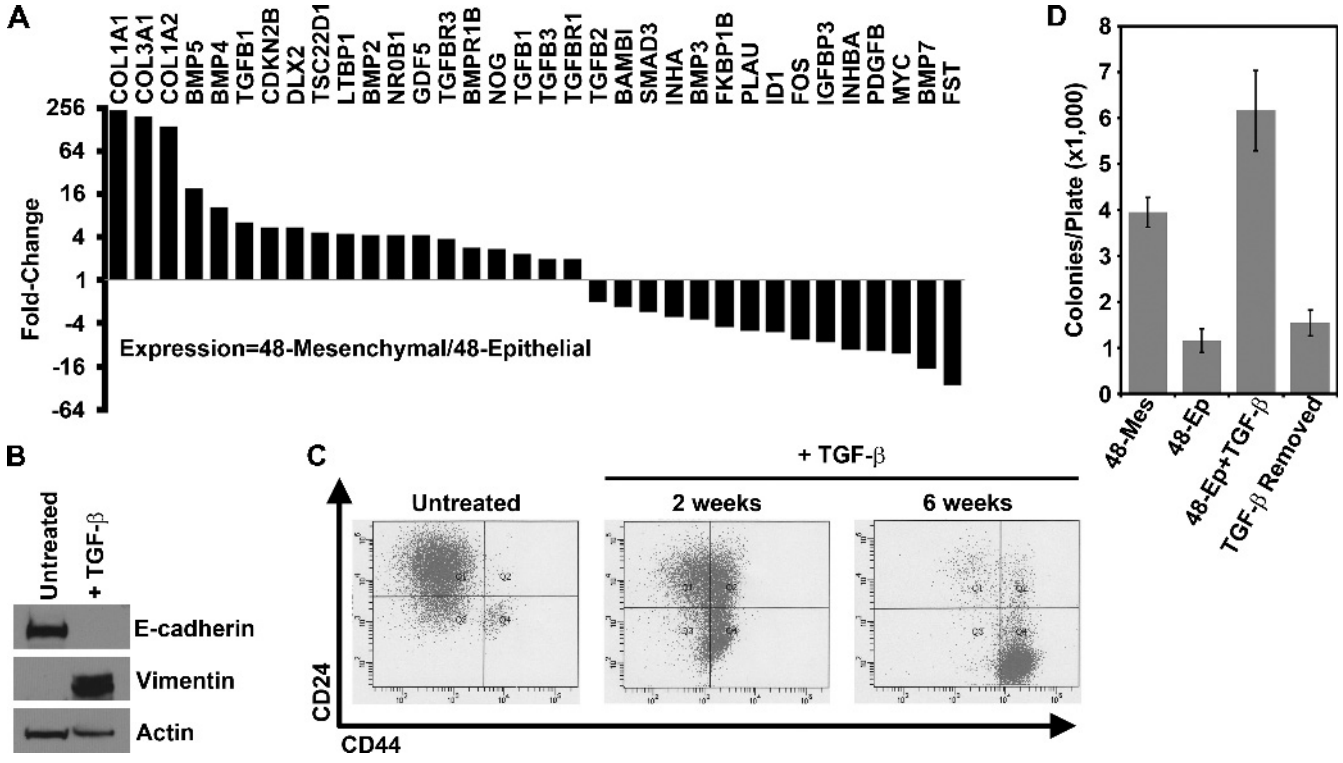


**Figure 5.** TGF-β drives EMT and acquisition of CSC properties. (A) Gene expression differences of 48-Mesenchymal compared to 48-Epithelial cells. 48-Epithelial cells exposed to exogenous TGF-β were analyzed by (B) Western blot, (C) flow cytometry, or (D) for AIG with 48-Mesenchymal cells (48-Mes) as a positive control. At the time of plating, TGF-β was removed from 48-Epithelial cells that were previously exposed (TGF-β Removed).

generated 48-Mesenchymal population is derived from an EMT driven at least partially by enhanced autocrine TGF-β signaling.

Tumor epithelial cells respond to aberrantly elevated cytokines, chemokines, and growth factors in the tumor microenvironment, which can be produced by the cancer cells themselves or a variety of tumor-associated stromal cells. We hypothesized that elevated TGF-β from the tumor microenvironment would also induce EMT in transformed HMECs generating a mesenchymal/CSC population. 48-Epithelial cells were treated with recombinant TGF-β1 to recapitulate elevated cytokine levels in the tumor microenvironment. TGF-β1 exposure increased vimentin protein, decreased E-cadherin protein, and induced the acquisition of a $CD24^-/CD44^+$ CSC profile (Figure 5, *B* and *C*). 48-Epithelial cells treated for 2 weeks with TGF-β1 were plated in soft agar for 2 weeks with or without sustained TGF-β1 treatment, and AIG was assessed. Consistent with the $CD24^-/CD44^+$ CSC profile of the 48-Epithelial cells treated continuously with TGF-β1, these cells grew efficiently in agar similar to positive control (48-Mesenchymal; Figure 5*D*). Interestingly, removal of TGF-β1 at the time of plating resulted in inefficient agar growth similar to negative controls (48-Epithelial; Figure 5*D*).

TGF-β ligand binds to TGFβRII and TGFβRI resulting in phosphorylation of TGFβRI. Phosphorylated TGFβRI induces phosphorylation of the receptor-associated SMAD2 or SMAD3 proteins, which can then complex with SMAD4 and translocate to the nucleus to affect gene expression. SMAD2/4 or SMAD3/4 complexes are inhibited by SMAD7. Alternatively, TGF-β can also activate TAK-1 [25–27]. We sought to determine whether exogenous TGF-β–induced EMT and generation of CSC required the TGF-β receptor complex, SMAD proteins, and/or TAK-1. 48-Epithelial cells were infected with retroviruses encoding DN-TGFβRII, DN–TAK-1, SMAD7, or vector control retroviruses. Analysis of CD24 and CD44 demonstrated that all 48-Epithelial derivatives retained a $CD24^+/CD44^-$ non-CSC surface marker profile and did not form colonies when tested for AIG, similar to the parental 48-Epithelial population (Figure 6*A*). Treatment with TGF-β1 induced a $CD24^-/CD44^+$ CSC population and AIG in the vector control and DN–TAK-1 derivatives, indicating that TAK-1 signaling was not required for the acquisition of CSC properties (Figure 6, *A* and *B*). In contrast, expression of DN-TGFβRII or SMAD7 efficiently suppressed the emergence of a $CD24^-/CD44^+$ population and AIG in response to TGF-β1 treatment (Figure 6, *A* and *B*). Taken together, these results suggest that TGF-β1 engages SMAD-mediated signaling to induce EMT and generate a mesenchymal/CSC population capable of AIG. Interestingly, these data also suggest that continuous TGF-β1 signaling is required for maintenance of mesenchymal/CSC populations.

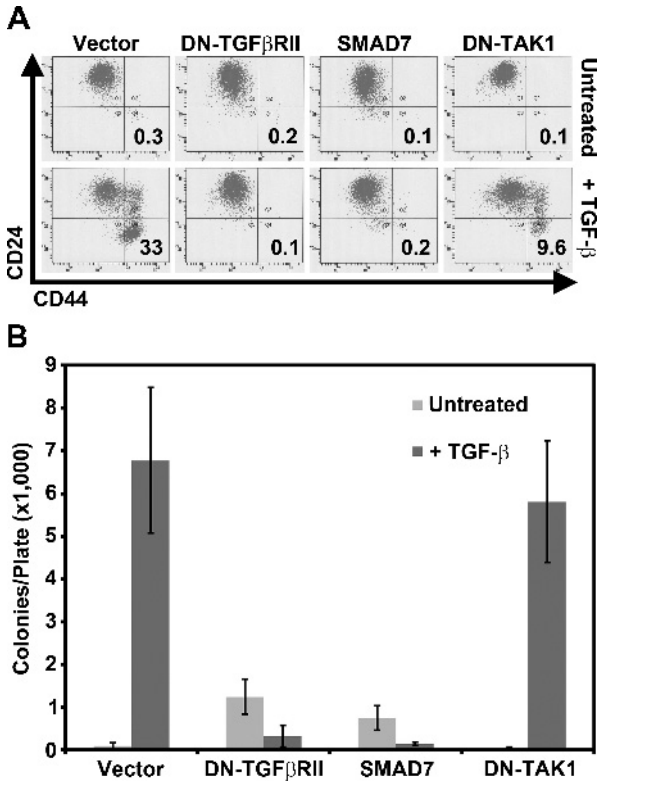


**Figure 6.** TGF-β–induced CSCs require receptor/SMAD signaling. 48-Epithelial cells expressing DN-TGFβRII, SMAD7, DN–TAK-1, or control cells (Vector) were analyzed by (A) flow cytometry with percent $CD44^+$ in the lower right corners or for (B) AIG before and after exposure to exogenous TGF-β.

### *Paracrine Cytokine Signaling Elicits Epithelial-Mesenchymal Plasticity*

Previous studies have determined that TGF-β–induced EMT of murine mammary epithelial cells requires activation of the PI3K-AKT-mTOR signaling pathway [28,29]. Indeed, the 48-Mesenchymal/CSC population that arose through spontaneous EMT harbored increased AKT protein phosphorylated at serine 473 indicative of mTOR activation. This suggests a potential therapeutic opportunity to target CSC within tumors by inhibiting TGF-β or PI3K-AKT-mTOR activation. Thus, we hypothesized that chemical inhibitors of the TGF-β and PI3K-AKT-mTOR signaling pathways would inhibit generation of CSC and AIG in response to exogenous cytokine exposure. The 48-Epithelial cells were treated for 2 weeks with TGF-β1 alone or in combination with the PI3K inhibitor LY, the mTOR inhibitor RAP, or the TGF-βRI inhibitor SB. As expected, treatment of 48-Epithelial cells with TGF-β1 for 2 weeks increased the $CD24^-/CD44^+$ CSC population from 5.9% to 28.7% (Figure 7*A*). Co-administration of TGF-β1 with LY or RAP led to 19.5% and 30.0% $CD24^-/CD44^+$ CSC, respectively, similar to TGF-β1 treatment alone (Figure 7*A*). However, co-administration of SB completely abrogated the ability of TGF-β1 to generate $CD24^-/CD44^+$ CSC populations (Figure 7*A*). This result suggests that specific inhibition of the TGF-β pathway, not PI3K-AKT-mTOR signaling, is capable of blocking EMT and CSC generation induced by microenvironmental TGF-β1.

Since our results suggested that continuous TGF-β exposure was required to sustain AIG, we hypothesized that mesenchymal/CSC generated by TGF-β conversion may also be reverted to epithelial/non-CSC by inhibiting the TGF-β signaling pathway. 48-Epithelial cells were treated for 3 weeks with TGF-β1 to generate mesenchymal/CSC. At 3 weeks, the treated cells were separated into the following three groups: 1) continued TGF-β1 treatment alone, 2) removal of TGF-β1, or 3) continued TGF-β1 treatment with co-administration of LY, RAP, or SB chemical inhibitors for 3 weeks. 48-Epithelial cells treated continuously with TGF-β1 for 6 weeks were 88.9% $CD24^-/CD44^+$ CSC (Figure 7*B*). Cells that were exposed for 3 weeks to TGF-β1 and then had it removed for 3 weeks were 33.5% $CD24^-/CD44^+$ CSC, with strongly suppressed AIG (Figure 7*B*). Cells treated with TGF-β1 for 3 weeks and then TGF-β1 together with LY, RAP, or SB for three additional weeks were 87.2%, 87.5%, and 43.2% $CD24^-/CD44^+$ CSC, respectively (Figure 7*B*). As described above,

LY or RAP was unable to suppress AIG, consistent with the inability of each of the inhibitors to decrease the $CD24^-/CD44^+$ CSC (Figure 7*C*). Treatment with SB suppressed both the $CD24^-/CD44^+$ CSC population and AIG, similar to the cells that had TGF-β1 removed (Figure 7, *B* and *C*). These data suggest that mesenchymal/CSC populations induced by TGF-β in the tumor microenvironment may be reverted to epithelial/non-CSC by inhibiting TGF-β signaling within these cells. Interestingly, the 48-Mesenchymal cells generated spontaneously during transformation by autocrine TGF-β signaling did not respond to type I receptor inhibition by SB (Figure 7, *D* and *E*).

## Discussion

Metastasis is the overwhelming cause of breast cancer patient mortality, yet our understanding of this complex problem remains limited. An emerging concept for metastasis is that cellular plasticity associated with EMT and subsequent mesenchymal-to-epithelial transition is critical for the ability of cancer cells to disseminate from the primary tumor site, survive circulation, and establish a growing tumor at a secondary site. Indeed, a population of pancreatic cells that exhibit EMT and stem cell properties was locally invasive and led to the presence of CTCs in the bloodstream even before frank malignancy could be observed [30]. Importantly, when the pancreatic cancer cells were separated on the basis of their epithelial or mesenchymal markers, each population produced similar mixed tumors and metastases. This study illustrates the importance of epithelial-mesenchymal plasticity as a tumor- and metastasis-promoting property. A recent study further supports a role for EMT in metastasis by demonstrating that breast CTCs are highly enriched for mesenchymal markers, and increases in circulating mesenchymal cells are associated with disease progression [31]. In contrast, breast cancer patient metastases typically reflect the primary tumor histologically, suggesting that circulating mesenchymal cells must revert to an epithelial state to promote metastatic outgrowth [32–34]. We report here a model of epithelial-mesenchymal plasticity that is generated by cooperation between intrinsic genetic changes within a developing cancer cell and exogenous, tumor microenvironmental cytokine signaling.

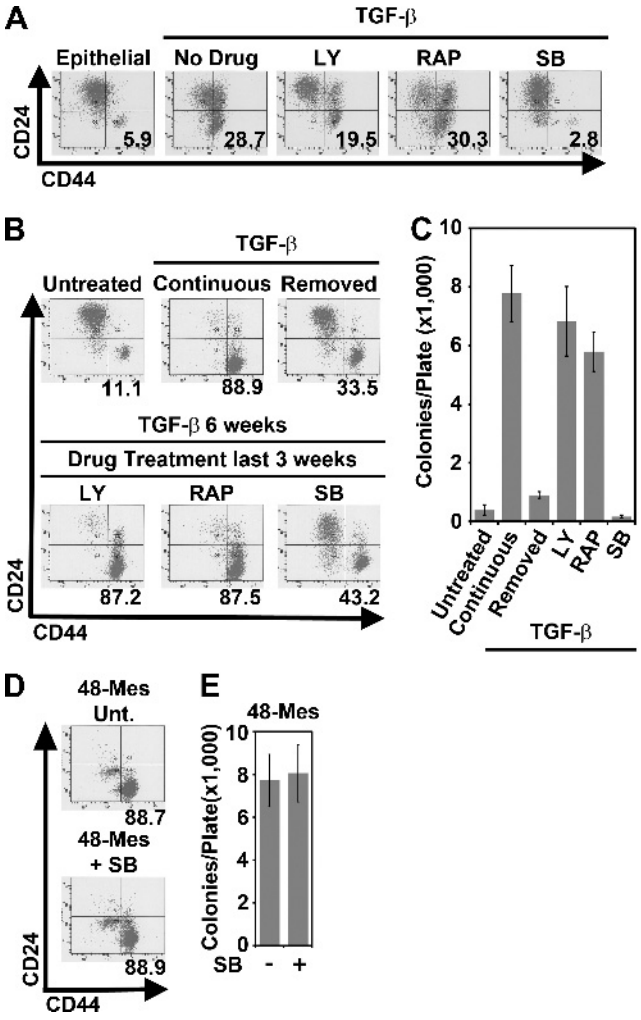


**Figure 7.** Epithelial-mesenchymal plasticity is induced by exogenous cytokine signaling. (A) 48-Epithelial cells exposed to TGF-β alone or in combination with inhibitors to PI3K (LY), mTOR (RAP), or TGFβRI (SB) were analyzed by flow cytometry. 48-Epithelial cells treated with TGF-β for 6 weeks (continuous), for 3 weeks, and then removed for 3 weeks (removed) or for 3 weeks and then in combination with LY, RAP, or SB for 3 weeks were analyzed by (B) flow cytometry with percent $CD44^+$ in the lower right corners and for (C) AIG. Spontaneous 48-Mesenchymal cells (48-Mes) were treated for 2 weeks with SB and analyzed by (D) flow cytometry or for (E) AIG.

Previously, we described a genetically defined, stepwise model of HMEC transformation and identified TGF-β signaling as a key regulator of RAS-mediated senescence in cells lacking p16 and p53 [18]. Once the cytostatic effects of TGF-β were dismantled by constitutive c-MYC expression, RAS-mediated transformation proceeded unchecked. Importantly, while constitutive c-MYC expression suppressed TGF-β–mediated senescence, it allowed the transformed HMECs to retain the TGF-β receptors and SMAD proteins responsible for inducing EMT, which we describe here. During stepwise transformation of HMECs, a subpopulation of mesenchymal-like cells was generated by spontaneous EMT (Figure 8*A*). The mesenchymal-like cells acquired properties associated with breast CSCs. Increased gene expression of several components of TGF-β, BMP, and WNT signaling was identified in the spontaneous mesenchymal/CSC population, suggesting that autocrine TGF-β signaling was at least partly responsible for the spontaneous EMT. The spontaneous mesenchymal/CSC did not respond to pharmacologic inhibition of TGF-β signaling and formed poorly differentiated tumors in immune-compromised mice, indicating that they are locked in a state associated with EMT and breast CSCs but are incapable of differentiating. Thus, spontaneous EMT does not demonstrate the epithelial-mesenchymal plasticity posited to be required for breast cancer metastasis.

Studies of the tumor interstitial fluid have identified more than 1000 proteins that have been secreted, externalized due to cell death, or shed by membrane vesicles into the breast tumor microenvironment [35]. Many of these proteins are secreted from the 20 or more different cell types that are present within the tumor stroma [36]. Cytokines top the list of tumor-associated secreted factors and are likely to have important effects on epithelial-mesenchymal plasticity. Our study alone has identified the potential involvement of WNT5A, GDF5, BMP2, BMP4, BMP5, TGF-β1, and TGF-β3 as potential regulators of EMT in our model. To explore the possibility that cytokines present in the tumor microenvironment influence epithelial-mesenchymal plasticity, transformed epithelial cells were exposed to TGF-β. Exposure to exogenous TGF-β increased AIG, induced EMT, and generated mesenchymal/CSC. Interestingly, removal of the exogenous TGF-β caused reversion of the mesenchymal/

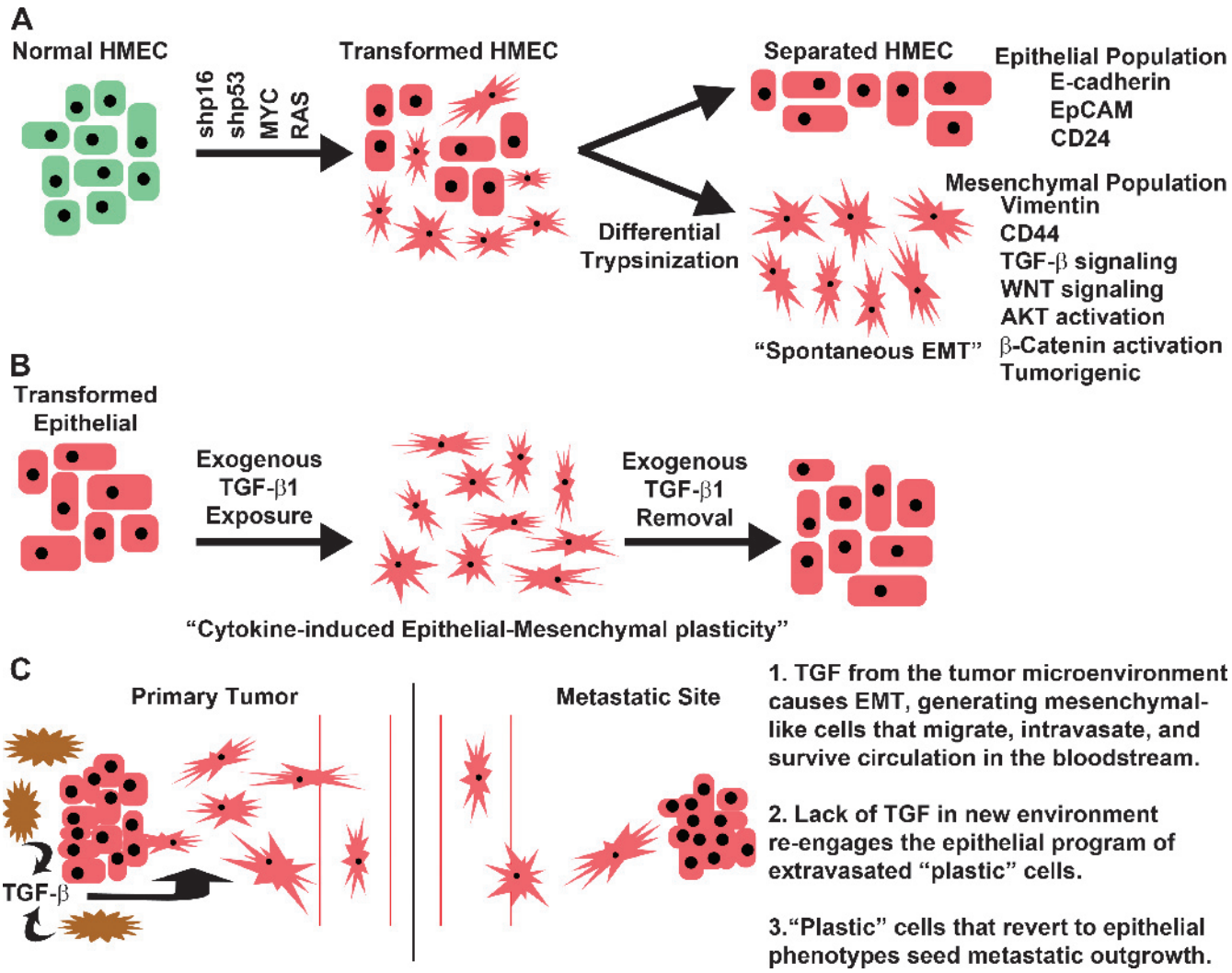


**Figure 8.** HMEC transformation generates spontaneous EMT and plastic cell populations. (A) Representation of the stepwise, genetically defined transformation protocol producing stable spontaneous EMT cells. Markers and properties of the isolated populations are listed. (B) Representation of the epithelial-mesenchymal plasticity identified in transformed epithelial populations by exogenous cytokine exposure. (C) Representation of the proposed role of epithelial-mesenchymal plasticity in metastasis induced by the tumor microenvironment.

CSC to epithelial/non-CSC, indicating that the CSCs become addicted to this key microenvironmental cue. Thus, epithelial-mesenchymal plasticity was generated by exposure and removal of exogenous TGF-β (Figure 8*B*). It is yet to be determined whether the myriad of other tumor-associated cytokines influences epithelial-mesenchymal plasticity. Our model can be used to define how signaling interactions between extrinsic and intrinsic factors influence epithelial tumor plasticity.

Our ultimate goal is to identify novel therapeutic strategies that inhibit the ability of tumor microenvironmental factors to induce epithelial-mesenchymal plasticity with hopes of diminishing a tumor's capacity to undergo metastasis. TGF-β signaling has been proposed as a therapeutic target, and TGF-β inhibitors are currently being developed for clinical use [37–39]. Indeed, disruption of canonical TGF-β receptor/SMAD signaling within fully transformed HMECs abrogated the ability of exogenous TGF-β to induce AIG and generate mesenchymal/CSC populations. Moreover, pharmacologic inhibition of TGF-β signaling in our plasticity model also decreased AIG and mesenchymal/CSC populations. This suggests that targeting TGF-β signaling, and potentially additional tumor-associated cytokine signaling, may be an effective strategy to inhibit generation of mesenchymal/CSC. Suppressing TGF-β signaling remains risky, as it is clearly involved in organismal homeostasis and is a crucial tumor suppressor early in cancer development. Therefore, we propose to use our model of epithelial-mesenchymal plasticity to identify novel tumor-associated cytokines that drive EMT and the acquisition of CSC properties. Identifying novel tumor-associated cytokines that regulate epithelial-mesenchymal plasticity and CSC properties is highly desirable, given their potential impact on metastatic outgrowth. By inhibiting the signaling pathways in tumor cells activated by exogenous cytokines from the tumor microenvironment, we may be able to block the generation of mesenchymal/CSC and subsequent tumor cell spread.

Our study demonstrates that exogenous cytokines present in the tumor microenvironment can cooperate with intrinsic genetic changes to produce epithelial-mesenchymal plasticity. If the key signals that regulate tumor cell plasticity originate from the tumor-associated stromal cells of the primary tumor, then CTCs that have traveled to secondary sites will encounter a significant shift in microenvironmental cues. As CTCs arrive at secondary sites where the original cytokine signal is no

longer present, only the cells that are capable of epithelial-mesenchymal plasticity will generate metastatic outgrowth (Figure 8*C*). As such, the cross talk between tumor epithelial and tumor-associated stromal cells may be an effective target for therapy to reduce metastasis. This may be accomplished by targeting the tumor epithelial cells themselves as described here or targeting the tumor-associated stromal cells that are producing the cytokine signals.

## References


[1] Nguyen DX, Bos PD, and Massagué J (2009). Metastasis: from dissemination to organ-specific colonization. *Nat Rev Cancer* **9**, 274–284.

[2] Fidler IJ (2003). The pathogenesis of cancer metastasis: the 'seed and soil' hypothesis revisited. *Nat Rev Cancer* **3**, 453–458.

[3] Boyer B and Thiery JP (1993). Epithelium-mesenchyme interconversion as example of epithelial plasticity. *APMIS* **101**, 257–268.

[4] Hay ED (1995). An overview of epithelio-mesenchymal transformation. *Acta Anat (Basel)* **154**, 8–20.

[5] Kalluri R and Neilson EG (2003). Epithelial-mesenchymal transition and its implications for fibrosis. *J Clin Invest* **112**, 1776–1784.

[6] Kalluri R and Weinberg RA (2009). The basics of epithelial-mesenchymal transition. *J Clin Invest* **119**, 1420–1428.

[7] Frixen UH, Behrens J, Sachs M, Eberle G, Voss B, Warda A, Löchner D, and Birchmeier W (1991). E-cadherin-mediated cell-cell adhesion prevents invasiveness of human carcinoma cells. *J Cell Biol* **113**, 173–185.

[8] Perl AK, Wilgenbus P, Dahl U, Semb H, and Christofori G (1998). A causal role for E-cadherin in the transition from adenoma to carcinoma. *Nature* **392**, 190–193.

[9] Yang J and Weinberg RA (2008). Epithelial-mesenchymal transition: at the crossroads of development and tumor metastasis. *Dev Cell* **14**, 818–829.

[10] Bastid J (2012). EMT in carcinoma progression and dissemination: facts, unanswered questions, and clinical considerations. *Cancer Metastasis Rev* **31**, 277–283.

[11] Gunasinghe NP, Wells A, Thompson EW, and Hugo HJ (2012). Mesenchymal-epithelial transition (MET) as a mechanism for metastatic colonisation in breast cancer. *Cancer Metastasis Rev* **31**, 469–478.

[12] Hanahan D and Weinberg RA (2011). Hallmarks of cancer: the next generation. *Cell* **144**, 646–674.

[13] Finak G, Bertos N, Pepin F, Sadekova S, Souleimanova M, Zhao H, Chen H, Omeroglu G, Meterissian S, Omeroglu A, et al. (2008). Stromal gene expression predicts clinical outcome in breast cancer. *Nat Med* **14**, 518–527.

[14] Mani SA, Guo W, Liao MJ, Eaton EN, Ayyanan A, Zhou AY, Brooks M, Reinhard F, Zhang CC, Shipitsin M, et al. (2008). The epithelial-mesenchymal transition generates cells with properties of stem cells. *Cell* **133**, 704–715.

[15] Al-Hajj M, Wicha MS, Benito-Hernandez A, Morrison SJ, and Clarke MF (2003). Prospective identification of tumorigenic breast cancer cells. *Proc Natl Acad Sci USA* **100**, 3983–3988.

[16] Junk DJ, Cipriano R, Stampfer M, and Jackson MW (2013). Constitutive CCND1/CDK2 activity substitutes for p53 loss, or MYC or oncogenic RAS expression in the transformation of human mammary epithelial cells. *PLoS One* **8**, e53776.

[17] Garbe JC, Bhattacharya S, Merchant B, Bassett E, Swisshelm K, Feiler HS, Wyrobek AJ, and Stampfer MR (2009). Molecular distinctions between stasis and telomere attrition senescence barriers shown by long-term culture of normal human mammary epithelial cells. *Cancer Res* **69**, 7557–7568.

[18] Cipriano R, Kan CE, Graham J, Danielpour D, Stampfer M, and Jackson MW (2011). TGF-β signaling engages an ATM-CHK2-p53–independent RAS-induced senescence and prevents malignant transformation in human mammary epithelial cells. *Proc Natl Acad Sci USA* **108**, 8668–8673.

[19] Brummelkamp TR, Bernards R, and Agami R (2002). A system for stable expression of short interfering RNAs in mammalian cells. *Science* **296**, 550–553.

[20] Abbott DW, Yang Y, Hutti JE, Madhavarapu S, Kelliher MA, and Cantley LC (2007). Coordinated regulation of Toll-like receptor and NOD2 signaling by K63-linked polyubiquitin chains. *Mol Cell Biol* **27**, 6012–6025.

[21] Tang B, de Castro CK, Barnes HE, Parks WT, Stewart L, Böttinger EP, Danielpour D, and Wakefield LM (1999). Loss of responsiveness to transforming growth factor β induces malignant transformation of nontumorigenic rat prostate epithelial cells. *Cancer Res* **59**, 4834–4842.

[22] Wang H, Song K, Krebs TL, Yang J, and Danielpour D (2008). Smad7 is inactivated through a direct physical interaction with the LIM protein Hic-5/ARA55. *Oncogene* **27**, 6791–6805.

[23] Scheel C, Eaton EN, Li SH, Chaffer CL, Reinhardt F, Kah KJ, Bell G, Guo W, Rubin J, Richardson AL, et al. (2011). Paracrine and autocrine signals induce and maintain mesenchymal and stem cell states in the breast. *Cell* **145**, 926–940.

[24] Morel AP, Lièvre M, Thomas C, Hinkal G, Ansieau S, and Puisieux A (2008). Generation of breast cancer stem cells through epithelial-mesenchymal transition. *PLoS One* **3**, e2888.

[25] Attisano L and Wrana JL (2002). Signal transduction by the TGF-β superfamily. *Science* **296**, 1646–1647.

[26] Derynck R and Zhang YE (2003). Smad-dependent and Smad-independent pathways in TGF-β family signalling. *Nature* **425**, 577–584.

[27] Shi Y and Massagué J (2003). Mechanisms of TGF-β signaling from cell membrane to the nucleus. *Cell* **113**, 685–700.

[28] Bakin AV, Tomlinson AK, Bhowmick NA, Moses HL, and Arteaga CL (2000). Phosphatidylinositol 3-kinase function is required for transforming growth factor β-mediated epithelial to mesenchymal transition and cell migration. *J Biol Chem* **275**, 36803–36810.

[29] Lamouille S and Derynck R (2007). Cell size and invasion in TGF-β–induced epithelial to mesenchymal transition is regulated by activation of the mTOR pathway. *J Cell Biol* **178**, 437–451.

[30] Rhim AD, Mirek ET, Aiello NM, Maitra A, Bailey JM, McAllister F, Reichert M, Beatty GL, Rustgi AK, Vonderheide RH, et al. (2012). EMT and dissemination precede pancreatic tumor formation. *Cell* **148**, 349–361.

[31] Yu M, Bardia A, Wittner BS, Stott SL, Smas ME, Ting DT, Isakoff SJ, Ciciliano JC, Wells MN, Shah AM, et al. (2013). Circulating breast tumor cells exhibit dynamic changes in epithelial and mesenchymal composition. *Science* **339**, 580–584.

[32] Chaffer CL, Thompson EW, and Williams ED (2007). Mesenchymal to epithelial transition in development and disease. *Cells Tissues Organs* **185**, 7–19.

[33] Chao YL, Shepard CR, and Wells A (2010). Breast carcinoma cells re-express E-cadherin during mesenchymal to epithelial reverting transition. *Mol Cancer* **9**, 179.

[34] Kowalski PJ, Rubin MA, and Kleer CG (2003). E-cadherin expression in primary carcinomas of the breast and its distant metastases. *Breast Cancer Res* **5**, R217–R222.

[35] Celis JE, Gromov P, Cabezón T, Moreira JM, Ambartsumian N, Sandelin K, Rank F, and Gromova I (2004). Proteomic characterization of the interstitial fluid perfusing the breast tumor microenvironment: a novel resource for biomarker and therapeutic target discovery. *Mol Cell Proteomics* **3**, 327–344.

[36] Egeblad M, Nakasone ES, and Werb Z (2010). Tumors as organs: complex tissues that interface with the entire organism. *Dev Cell* **18**, 884–901.

[37] Connolly EC, Freimuth J, and Akhurst RJ (2012). Complexities of TGF-β targeted cancer therapy. *Int J Biol Sci* **8**, 964–978.

[38] Elliott RL and Blobe GC (2005). Role of transforming growth factor beta in human cancer. *J Clin Oncol* **23**, 2078–2093.

[39] Yingling JM, Blanchard KL, and Sawyer JS (2004). Development of TGF-β signalling inhibitors for cancer therapy. *Nat Rev Drug Discov* **3**, 1011–1022.